

Industrial waste materials as adsorbents for the removal of As and other toxic elements from an abandoned mine spoil heap leachate: a case study in Asturias

Authors: Julia Ayala¹, Begoña Fernández^{1, 2},

1- Laboratorio de Metalurgia. Escuela de Minas Energía y Materiales. Universidad de Oviedo. Independencia 13. 33004. Oviedo. Spain.

2 corresponding autor .Tel: + 34 985104235

Email: fernandezbegona@uniovi.es; jayala@uniovi.es

Abstract

The purpose of this study is to determine the capacity of four industrial waste materials originate from steelmaking processes (slags) and from gas treatment at a thermal power plant (fly ash and gypsum) to remove As and other contaminants from a leachate from the spoil heap of an abandoned mercury mine. Arsenic removal is faster in the first minutes, then increases only slightly over time reaching equilibrium in 8 hours. As removal efficiency increased with increasing adsorbent concentration. As removal efficiency was found to be 82.7%, 71%, 37.2% and 27.2% for EA, FA, HA and G, respectively, when employing 80 g/dm³ of adsorbent concentration. The main mechanism of As removal appears to be the **formation of As - Ca compounds**. The results show that Hg and Pb are completely removed using low concentrations of adsorbents regardless of the waste material used in the treatment. FA removed more than 82% of other toxic elements such as Ni, Cu and Cd. EA is the most effective byproduct of the four employed in this study for removing pollutants, while G is the least effective. The present study shows it is possible to carry out an efficient and economical treatment of mine leachate using these byproducts.

Keywords

Arsenic removal, Mercury mine waste, Industrial byproducts, Adsorption, Water pollution

1. Introduction

Arsenic occurs naturally in soil and minerals. It can be released to the atmosphere from natural source such as volcanoes and also wind-blown soil, or released from anthropogenic source such as coal combustion, electronic components, nonferrous metal mining and metallurgical processing to obtain these metals. Released arsenic is usually attached to very small particles (Singh et al.2015, Wu et al. 2017).Arsenic may be released to water by leaching soil, minerals and industrial waste materials such as mining and metallurgical waste. The mobility of arsenic depends on pH and redox

potential, which have a major influence on adsorption/desorption processes and precipitation/dissolution processes (Filippi et al. 2015, Haffert and Craw 2008).

Rieuwerts et al. 2014 studied the role of mineralogy in the mobility and environmental impact of As in mine waste and stream sediments in the Tamar Valley. These authors found that the potential mobility of arsenic from mine waste was highly variable, ranging from 0.4% to 51.4% of the total As. In natural water, the predominant species under reducing conditions is As (III) and under oxidizing conditions, As (V). Furthermore, As (III) is more toxic than As (V). The concentration of arsenic in natural surface water and groundwater is generally around $1 \mu\text{g}/\text{dm}^3$, but may exceed $1000 \mu\text{g}/\text{dm}^3$ in contaminated areas or where arsenic levels in soil are high (ATSDR).

Typical arsenic concentrations for uncontaminated soil range from 1 to $40 \mu\text{g}/\text{g}$. However, these values can increase considerably in polluted mine soil, such as at the Barruecopardo mine in Salamanca (Spain): $177 \mu\text{g}/\text{g}$ (Álvarez-Ayuso et al. 2016), in the Shimen realgar mine area in China: $5240 \mu\text{g}/\text{g}$ (Wan et al. 2017) and in the municipality of Huelva (Spain): $2066 \mu\text{g}/\text{g}$ (Guillén et al. 2012).

Mine workings and mercury processing activities constitute an important source of arsenic contamination. A major problem exists with abandoned mercury mines, as both the work at the mining and metallurgical facilities was carried out without any environmental control, the waste being accumulated in spoil heaps.

This paper focuses on La Soterraña abandoned mine. La Soterraña mine ($-5^{\circ}50'28''$ longitude, $43^{\circ}11'48''$ latitude) is close to the village of Muñón Cimero (600 m) and is located approximately 5 km from the town of Pola de Lena, (11 430 inhabitants in 2016), both in Asturias, northwestern Spain, Fig 1.

Mining works began in 1842, with essentially surface excavations on old sites considered to date from the Roman era. In 1948, the Minas de la Soterraña S.A. company was established and a new procedure was introduced to obtain Hg and As_2O_3 , the most productive stage starting with simultaneous improvements in mining production and the metallurgical facilities. The consumption of mercury decreased at the beginning of the 1970s, leading to the closure of the works in 1974.

La Soterraña ore paragenesis comprises cinnabar (HgS), realgar (AsS), at a much lower proportion, orpiment (As_2O_3), pyrite (FeS_2) and marcasite (FeS_2), the presence of pararealgar (AsS) also being common in surface areas as a product of alteration of realgar (Luque and Gutierrez, 2006).

At La Soterraña mine, the emissions of particulate pollutants, the dumping of mining waste and waste from the metallurgical facility, as well as the contaminated water, affected a large area of around $80\,000 \text{ m}^2$ (Luque 1985). La Soterraña spoil heap is cataloged in the Principality of Asturias inventory of contaminated soils with the site code 3303303. Most of the material that constitutes the spoil heap came from the different mercury and arsenic extraction processes www.Asturias.es.

Climatic features in Asturias comprise mild winters, temperate summers, humid air, abundant cloudiness and frequent rainfall in all seasons, with average annual rainfall values ranging between 827 and 1787 mm, with an average of 1296 mm. The annual distribution of rainfall is relatively homogeneous, with two maximums in spring and autumn and a summer minimum, www.chcantabrico.es.

Rainwater and runoff waters percolate through spoil heap materials and the rest of the facility, dissolving and mobilizing contaminated material. These pollutants can pass into a small stream, located on one side of the mine, which flows into the Lena River, a tributary of the Caudal River, which eventually flows into the Nalón River, which is the main river in the region.

[Matanzas et al. 2017](#) studied the geochemistry of the La Soterraña soil waste system and determined that the As concentration was very high, reporting that more than 95% of the total As of the spoil heap was in the form of As(V). The percentage of arsenic soluble in water reported by [Larios et al. 2012](#) at La Soterraña varies between 4.5 and 7.6% of the total As present in the sample.

Several treatments have been reported for removing As and heavy metals from contaminated water: coagulation/flocculation, electrocoagulation, phytoremediation, bioremediation, ion exchange and adsorption, among others ([Dil et al. 2017](#), [Gil-Díaz et al. 2017](#), [Hayat et al. 2017](#), [Mazaheri et al. 2017](#), [Ebrahim et al. 2017](#), [Nicomel et al. 2015](#), [Rahman et al. 2014](#), [Sarkar and Paul 2016](#), [Ungureanu et al. 2015](#), [Vidheesh and Singh 2017](#)).

Several articles have been published on the removal of As from water using different adsorbents such as steelmaking waste ([Ahn, et al. 2003](#), [Chakraborty et al. 2014](#), [Oh et al. 2012](#)), magnesia-loaded fly ash ([Li et al. 2012](#)), coal fly ([Balsamo et al 2013](#), [Medina et al. 2010](#), [Wang and Tsang 2013](#)), iron oxides ([Aredes et al. 2013](#), [Dai et al. 2016](#), [Yang et al. 2017](#), [Gimenez et al. 2007](#), [Mamindy-Pajany et al. 2011](#)), clays among others ([Bentahar et al. 2016](#), [Mukhopadhyay et al. 2017](#)).

Most reports published to date on the As removal by byproducts have used synthetic waters with a low As content. In the present study, however, a leachate with a high content in As and other contaminants was treated.

The aim of this research was to study, at the laboratory level, the use of industrial waste materials as adsorbents for As removal and other toxic elements present in the leachate from abandoned mines. In a subsequent study, the intention is to carry out a pilot remediation study on the actual site.

2. Materials and methods

2.1 Materials

In this study, waste material from La Soterraña mine which contains significant amounts of As and four waste materials from local industries were used. The waste materials or byproducts from steelmaking processes (slag materials) and gas treatment at a thermal power plant (fly ash and gypsum) were used as adsorbents of As.

The La Soterraña waste (WA) and the other waste materials were dried at room temperature in order to minimize the loss of volatile contaminants. Fly ash (FA) and gypsum (G) were in the form of fine powders. The slag materials (EA and HA) were large in size, ranging between 10 and 15 cm, and hence were crushed using a jaw crusher and subsequently sieved through a 2-mm aperture screen before use. A fraction of the five solids was milled to a particle size of $< 100 \mu\text{m}$ to determine their chemical composition and pH. X-ray fluorescence (Phillips PW2404) was used to determine the major elements, while the quantification of the trace elements was performed by mass spectrometry with inductively coupled plasma (ICP-MS Agilent 7700) prior to dissolution with aqua regia using an Anton Paar 3000 microwave system.

The pH value of the samples was measured using a Eutech pH 2700 meter in a 1:2.5 (w/v) sample/water mixture after equilibrating for 30 min. In addition, the content of dissolved Ca, Mg and Fe in the supernatant liquid from the byproducts was determined by atomic absorption spectroscopy (Perkin Elmer AAnalyst 200).

The mining waste and byproducts were screened to give different particle sizes. The real density of the waste was determined using the pycnometer method (UNE Standard 80105), employing water as the immersion liquid.

The mineral composition of the byproducts was analyzed by X-ray diffraction (PANalytical X'Pert Pro MPD with $\text{CuK}\alpha$ radiation). The diffractometer was operated at 45 kV and 40 mA, over the range of 2θ from 5° to 90° , with a detector speed of $1^\circ/\text{min}$.

2.2. Leaching of the La Soterraña waste

The total arsenic present in the waste can be found in different forms: some are soluble in water (arsenate and weakly adsorbed species), soluble in Na_2HPO_4 (strongly adsorbed onto mineral surfaces), soluble in NH_4F (associated with Al oxyhydroxides), soluble in $\text{Na}_4\text{P}_2\text{O}_7$ (As bound to organic matter), soluble in ammonium oxalate/oxalic acid (As associated with amorphous Fe oxyhydroxides), soluble in bicarbonate and ascorbic acid (associated with poorly crystalline Fe hydroxide) and acid digestion in a microwave oven with HCl and HNO_3 (As co-precipitates with refractory minerals), [Larios et al. 2012](#).

A leachate was prepared to study whether the different byproducts may be able to minimize the As content that is solubilized by the percolation of rainwater on abandoned mine waste. The La Soterraña waste was leached according to European standard test EN 12457-4 by mixing the waste with deionized water (W:V ratio = 1:10) and shaking (10 rpm) at room temperature for 24 h in a

vertical rotary shaker. The leachate was then filtered and the pH, redox potential and conductivity were measured using a Eutech pH 2700 meter and EC-Meter BASIC 30 meter, respectively. As and heavy metal concentrations were determined by ICP.

2.3. Batch adsorption experiments

To study the ability of the byproducts to remove the As present in the leachate, batch adsorption tests were carried out at room temperature (20°C). Several researchers have found that the pH of the solution affects As removal (Ungureanu et al. 2015). In this study, the leachate was not previously conditioned, as the aim was to obtain as simple and as cheap a treatment as possible.

First, 100 cm³ polyethylene bottles containing the byproducts and La Soterraña leachate, employing an adsorbent concentration of 10 g/dm³, were shaken for different times ranging from 0.08 to 8h, subsequently separating the supernatant by filtration through a Watman114 filter. The pH, potential redox, conductivity and concentrations of As and other heavy metals were measured in the supernatant.

All experiments were performed in duplicate and the mean values were taken.

The percentage As removal efficiency was determined according to Eq. (1):

$$\% As_{removal} = \frac{C_o - C_e}{C_o} \times 100 \quad (1)$$

where C_o and C_e are respectively the As concentration (mg/dm³) before and after treatment.

The effect of dosage was studied by shaking La Soterraña leachate with different doses of byproducts, ranging from 10 to 80 g/dm³, for 8 h.

The surface morphology of the byproducts after treatment was investigated under a scanning electron microscope (SEM) and the qualitative element composition was analyzed using energy dispersive X-ray spectroscopy (EDX) (JEOL JSM 5600).

3. Results and discussion

3.1. Characterization of arsenic waste and byproducts

The chemical composition data on the arsenic waste (AW) and the four byproducts are presented in Table 1. The arsenic waste is mainly composed of SiO₂ (61.7%), Al₂O₃ (7.1%) and SO₃ (7.2%). It also has a high content in toxic elements, such as As (54 801 mg/Kg) and Hg (34 691 mg/kg), these contents being higher than those reported by Larios et al. 2012 (10 800 mg/Kg As and 1330 mg/Kg Hg) for La Soterraña mining waste. This difference may be due to the fact that the material used in this study comes from the furnaces area, while the material reported by Larios comes from upstream of the spoil heaps and the mining works. Gil-Díaz et al. 2017 found As values of 70 200 and 25 900 mg/Kg in another abandoned mine, El Terronal, also located in Asturias.

More than 80% of FA is SiO₂ and Al₂O₃, the content of these oxides being much lower in the other byproducts. The slag materials have a high content in CaO: 42% for EA and 38.3% for HA. Gypsum has small amounts of heavy metals. The As content present in the byproducts is relatively low: 59 mg/Kg for FA and 37.8 mg/Kg for HA, [Table 1](#).

The arsenic waste has a 5.1 pH value, the slightly acidic pH being mostly due to the oxidation of the sulfur compounds present in the spoil heap, while the pH values of the byproducts vary between 7.8 and 11.3. The contents of Ca, Mg, Fe in the supernatant liquid were determined, finding concentrations of 70 mg/dm³, 25.2 mg/dm³ and 30 mg/dm³ Ca and 3.3 mg/dm³, 2.9 mg/dm³ and 2.3 mg/dm³ Mg for EA, HA and FA, respectively. The concentration of Fe was < 0.1mg/dm³ in all cases. The strong alkalinity of the FA, EA and HA samples is due to the free Ca they contain.

The particle size of the byproducts used in this study is much smaller than that of the La Soterraña waste, [Fig 2](#). It can be seen that the waste materials from gas treatment at the thermal power plant are very fine in size, more than 90% being less than 63 microns, with d₅₀ = 45 microns and d₅₀ < 32 microns for the fly ash and gypsum, respectively, [Fig 2 b](#). The fraction of the slag materials smaller than 2 mm used in this study presents a very similar particle size, HA being slightly finer, with d₅₀ = 450 microns, [Fig 2c](#).

The XRD pattern reveals that the major crystalline phases present in the Fly ash were Mullite (Al₆Si₂O₁₃) and Quartz (SiO₂), while the minority phases were Maghemite (γ-Fe₂O₃), Gypsum (CaSO₄·2H₂O), Anhydrite (CaSO₄) and probably α-Fe, [Fig 3](#). The other byproduct from the thermal power plant is composed of Gypsum (CaSO₄·2H₂O) and small amounts of calcite (CaCO₃).

Regarding the slag materials: EA would be constituted mainly by Akermanite (Ca₂Mg(Si₂O₇)) and Larnite (Ca₂SiO₄), with Gypsum and Srebrodolskite (Ca₂Fe₂O₅) being the minor phases. The existence of Calcite, Hematite (α-Fe₂O₃) and Silimanite (Al₂SiO₅) is also likely. The minerals present in the HA slag are even more numerous, the following being identified: Calcite, Srebrodolskite, Larnite, Akermanite, Merwinite (Ca₃Mg (SiO₄)₂) and Magnetite (Fe₃O₄) as the majority phases, Lime (CaO) and Portlandite (Ca(OH)₂) as the minority phases, and possibly Quartz and Wustite (FeO).

3.2. Leaching of the La Soterraña waste

The leachate obtained according to standard test EN 12457-4 has a pH of 5.24, 196.8 mV redox potential and 2.2 mS/cm conductivity. The analysis performed by mass spectrometry with inductively coupled plasma shows a high content in As (59 056 μg/dm³) and much smaller amounts of heavy metals such as Hg, Ni, Zn, Cu, Cd and Pb, [Table 2](#). About 1% of the arsenic present in the waste was solubilized during the test. It should be noted that although the residue from mercury production has high concentrations of As and Hg, 54 801 mg/Kg and 34 691 mg/Kg, respectively, their mobility

is small. This indicates that most of the As and Hg are more tightly bound and would need a stronger reactant than water to be dissolved.

3.3. Batch adsorption experiments

3.3.1 Effect of contact time

Figure 4a shows that the rate of uptake of arsenic increases with increasing contact time between the leachate and the byproducts, the reaction being faster in the first minutes and subsequently increasing only slightly over time. In the tests performed with FA, 12.7% of the As was removed after 5 minutes, the removal efficiency reaching 21% after 8 hours. Similar values were found when the slag materials were used. However, the efficiency in the removal of arsenic with gypsum was lower, being only 13.1% after 8 hours.

The adsorption capacities of various adsorbents reported in some recent papers are summarized in Table 3. The experimental data of the present investigation may be comparable or even better than the values reported in the literature.

Figure 4b shows that, regardless of the reaction time, the pH obtained after the treatment with gypsum has a value close to 6. However, a progressive increase in pH was observed when the leachate was treated with other byproducts. This is due to the fact that the slag materials have a higher proportion of alkaline earth metals, which can become partially dissolved upon contact with the leachate, which is slightly acidic.

There is a decrease in the redox potential due to the oxidation reactions that occur when the leachate comes into contact with the slag materials, probably due to the oxidation of iron and iron oxides, Fig 4c. However, the conductivity increased slightly from 2.2 mS/cm before treatment to 2.3 mS/cm or 2.4 mS/cm after the adsorption tests in all cases.

3.3.2 Effect of the adsorbent dosage

The efficiency of As removal by the adsorbents increased with increasing adsorbent concentration. When the adsorbent concentration increases from 10 to 80 g/dm³, the removal efficiency varies from 19.3% to 82.7% for EA slag, while for FA it varies from 21% to 71%. Minor variations were found when the other two byproducts were used, Fig. 5a.

The final pH after the treatment with gypsum is close to neutral. However, with the other three byproducts, the alkalinity increases with increasing amounts of byproduct used in the treatment, Fig 5b. According to the Eh-pH diagrams of the As-O-H system, HAsO₄²⁻ is the predominant species in the 7-10 pH range, reached after the treatment with the different byproducts (Takeno 2005).

Most reported research has been carried out with synthetic waters. However, the results that may be obtained when treating wastewater can be very different as real waters contain a lot of ions and other substances that may increase or, in most cases, decrease the amount of arsenic retained by the adsorbents. [Chakraborty et al. 2014](#) found that the presence of silica and dissolved phosphates can decrease the removal of arsenic because these species can be adsorbed by the slag surface, thereby leaving fewer sites free for the removal of arsenic. They also found that the presence of dissolved calcium carbonate improves the removal of arsenic due to co-precipitation. [Wang et al. 2013](#) found that, in addition to silica and phosphates, the humic acid present in the wastewater also decreases the efficiency of arsenic removal.

Several researchers propose the following arsenic removal mechanisms from aqueous solutions: adsorption onto the surface and inside the pores of iron oxides and iron hydroxides and aluminum ([Dai et al. 2016](#), [Giles et al. 2011](#), [Gimenez et al. 2007](#), [Goldberg and Johnston 2011](#), [Mamindy-Pajany et al. 2011](#), [Siddiqui and Chaudhry 2017](#)), and precipitation of calcium and arsenic compounds ([Ahn et al. 2003](#)) or Ca-Fe-AsO₄ compounds ([Bluteau et al. 2009](#)). Different Ca-As compounds can be obtained depending on the molar Ca/As ratio and the pH, the precipitation of Ca-As compounds being favored by increasing the pH ([Bothe and Brown 1999](#), [Zhu 2006](#)).

[Ahn et al. 2003](#) conducted different experiments using various waste materials from steelmaking to treat a 25 mg/dm³ synthetic solution of As (V). They found that, in most of the waste materials used, As removal was due to the formation of Ca-As compounds rather than adsorption on iron oxides, the high concentration of calcium in solution providing a high pH (pH 12) that promotes the formation of Ca₄(OH)₂(AsO₄)₂ · 4 H₂O. [Chakraborty et al. 2014](#) propose two mechanisms: adsorption in the active sites due to the presence of free iron and iron oxides, and co-precipitation in arsenic removal using slag.

[Wang et al. 2013](#) used fly ash from a thermal power plant to remove arsenic from a synthetic solution containing a concentration of 0.8 mg/dm³ As. The efficiency in the removal of arsenic varied from 83% to 91% depending on the experimental conditions. The fly ash that they used had a high CaO content (35%). These authors propose both mechanisms: Fe and Al oxides/hydroxides have a large surface area with abundant hydroxyl groups capable of adsorbing the As (V), and the calcium that dissolves leads to precipitation of arsenic and calcium compounds.

[Fig 6](#) shows the morphology of the byproducts after leachate treatment and EDX analysis. EA and HA showed angular shapes, while FA and G presented more rounded shapes. According to EDX analysis, the As removal mechanism depends on the type of waste used. In the case of EA slag, it seems that the formation of As - Ca compounds takes place, while for HA and FA, the mechanism could be both adsorption by the iron compounds and precipitation of Ca - As compounds.

Gypsum is the byproduct that removes the least As. This may be because the mechanism in this case is solely precipitation of As - Ca compounds, there being no iron or aluminum compounds that

can adsorb this element. When gypsum is placed in contact with the leachate, some gypsum dissolves, a part of the released calcium reacting with the arsenate dissolved in the leachate (Chen et al. 2014, Rodríguez-Blanco et al. 2007, Zhang et al. 2015).

Fig. 7 shows the SEM-EDX analysis and the EDX elemental mapping of As after treating the leachate with EA. It can be seen that As is retained on the surface of the EA particles forming Ca-As compounds.

Leachate from the spoil heap materials is contaminated with other toxic elements, the concentration of these being very small compared to the concentration of arsenic: only 0.98 $\mu\text{g}/\text{dm}^3$, 47.5 $\mu\text{g}/\text{dm}^3$, 288.6 $\mu\text{g}/\text{dm}^3$, 107 $\mu\text{g}/\text{dm}^3$, 10.9 $\mu\text{g}/\text{dm}^3$ and 25.1 $\mu\text{g}/\text{dm}^3$ for Hg, Ni, Cu, Zn, Pb and Cd, respectively. The treatment of the leachate with byproducts led not only to a decrease in arsenic concentration, but also decreased the amounts of other toxic elements. The results show that Hg and Pb are completely removed regardless of the adsorbent concentration used in the treatment. FA removed more than 82% of the other pollutants, Fig 8. Zn removal practically does not depend on the amount of FA used. However, the removal of Ni, Cu and Cd increases with increasing amounts of adsorbent.

4. Conclusions

In this study, four byproducts were used in the adsorbent treatment of a leachate from an abandoned mercury mine. The adsorbents come from steelmaking processes (slag materials) and from gas treatment at a thermal power plant (fly ash and gypsum).

Based on the experimental results of this study, the following conclusions can be drawn:

Arsenic removal increases with increasing contact time between the leachate and byproducts, the reaction being faster in the first minutes, subsequently increasing only slightly over time. Kinetic studies suggest that equilibrium is reached within 8 hours.

The efficiency in As removal gradually increases as the dose of adsorbent increases from 10 to 80 g/dm^3 . Removal efficiencies of 82.7% and 71% were found for EA and FA, respectively, when using 80 g/dm^3 adsorbent. Minor variations were found when HA and G were used, 37.3% and 28.0%, respectively.

FA and HA remove As via two mechanisms: adsorption of arsenate ions on the active sites of the Fe and Al oxides/hydroxides of the byproducts, and precipitation of Ca-As compounds due to the solubilization of Ca ions that leads to an increase in pH. For EA and G, however, only the precipitation of As-Ca compounds is proposed.

The concentrations of other contaminants in the leachate also decreased after treatment with the byproducts, Hg and Pb being completely removed regardless of the adsorbent concentration used in the treatment. FA removed more than 82% of Zn^{2+} , Cd^{2+} , Cu^{2+} and Ni^{2+} , however metals removal

efficiency were within 65%-86% range for EA. Gypsum was found to be the least effective adsorbent, although it removed 72% of Cu^{2+} and more than 44% of Zn^{2+} , Cd^{2+} and Ni^{2+} .

All of the foregoing indicates that the four byproducts can be used in the treatment of mine leachate, being effective in simultaneously removing several pollutants such as As, Hg, Pb, Cu, Ni, Zn and Cd.

Finally, the environmental improvements obtained with the proposed method: decrease in the concentration of pollutants present in the water and the reuse of industrial waste from the steel and energy industries, shows that it is possible to carry out an efficient and economical treatment of mine leachate using these byproducts.

In a subsequent study, a pilot remediation study is conducted on the actual site.

Acknowledgements This work has been supported by project UE-17-SUBRPRODUCTS-LIFE16-481 financed by (UE) European Union.

References

- Agency for Toxic Substances and Disease Registry (ATSDR). Toxicological Profile for Arsenic. Available online: <http://www.atsdr.cdc.gov/ToxProfiles/tp.asp?id=22&tid=3> (accessed on 16/11/2017).
- Álvarez-Ayuso E., Abad-Valle P., Murciego A., Villar-Alonso P. 2016. Arsenic distribution in soils and rye plants of a cropland located in an abandoned mining area. *Sci. Total Environ.* 542, 238–246. <https://doi.org/10.1016/j.scitotenv.2015.10.054>.
- Ahn J. S., Chon C.-M., Moon H.-S., Kim K.-W. 2003. Arsenic removal using steel manufacturing byproducts as permeable reactive materials in mine tailing containment systems. *Water Res.* 37, 2478–2488. [https://doi.org/10.1016/S0043-1354\(02\)00637-1](https://doi.org/10.1016/S0043-1354(02)00637-1).
- Aredes S., Klein B., Pawlik M. 2013. The removal of arsenic from water using natural iron oxide minerals. *J. Clean Prod.* 60, 71 -76. <https://doi.org/10.1016/j.clepro.2012.10.035>.
- Balsamo M., Di Natale F., Erto A., Lancia A., Montagnaro F., Santoro L. 2010. Arsenate removal from synthetic wastewater by adsorption onto fly ash. *Desalination* 263, 58–63. <https://doi.org/10.1016/j.desal.2010.06.035>.

- Bentahar Y., Hurel C., Draoui K., Khairoun S., Marmier N. 2016. Adsorptive properties of Moroccan clays for the removal of arsenic (V) from aqueous solution. *Appl Clay Sci* 119, 385–392. <https://doi.org/10.1016/j.clay.2015.11.008>.
- Bothe J. V. Jr, Brown P.W. 1999. Arsenic immobilization by calcium arsenate formation. *Environ Sci. Technol.* 33, 3806-3811.
- Bluteau M.C., Becze L., Demopoulos G.P. 2009. The dissolution of scorodite in gypsum-saturated waters: Evidence of Ca–Fe–AsO₄ mineral formation and its impact on arsenic retention. *Hydrometallurgy* 97, 221–227. <https://doi.org/10.1016/j.hydromet.2009.03.009>.
- Chakraborty A, Sengupta A, Bhadu MK, Pandey A, Mondal A. 2014 . Efficient removal of arsenic (V) from water using steel-making slag. *Water Environ Res.*, 86 (6), 524-31. <https://doi.org/10.2175/106143014X13975035524907>.
- Chen X., Yang L., Zhang J., Huang Y. 2014. Exploration of As(III)/As(V) Uptake from Aqueous Solution by Synthesized Calcium Sulfate Whisker. *Chin. J. Chem. Eng.*, 22, 1340–1346. <https://doi.org/10.1016/j.cjche.2014.09.018>.
- Dai M., Xia L., Song S., Peng C., Lopez-Valdivieso A. 2016. Adsorption of As (V) inside the pores of Porous hematite in water. *J. Hazard. Mater.*, 307, 312- 317. <https://doi.org/10.1016/j.jhazmat.2016.01.008>.
- Dil E.A., Ghaedi M., Ghezelbash G. R., Asfaram A., Purkait M.K. 2017. Highly efficient simultaneous biosorption of Hg²⁺, Pb²⁺ and Cu²⁺ by Live yeast *Yarrowia lipolytica* 70562 following response surface methodology optimization: Kinetic and isotherm study. *J. Ind. Eng. Chem.*, 48 162-172. <https://doi.org/10.1016/j.jiec.2016.12.035>
- Filippi M., Drahota P., Machovič V., Böhmová V., Mihaljevič M. 2015. Arsenic mineralogy and mobility in the arsenic-rich historical mine waste dump. *Sci. Total Environ.* 536, 713–728. <https://doi.org/10.1016/j.scitotenv.2015.07.113>.
- Gil-Díaz M., Alonso J., Rodríguez-Valdés E., Gallego J.R., Lobo M.C. 2017. Comparing different commercial zero valent iron nanoparticles to immobilize As and Hg in brownfield soil. *Sci. Total Environ.* 584-585, 1324-1332. <https://doi.org/10.1016/j.scitotenv.2017.02.011>.

- Giles D.E., Mohapatra M., Issa T.B., S. Anand, Singh P. 2011. Iron and aluminium based adsorption strategies for removing arsenic from water. *J. Environ. Manage*, 92, 3011-3022. <https://doi.org/10.1016/j.jenvman.2011.07.018>.
- Gimenez J., Martínez M., de Pablo J., Rovira M.I., Duro L. 2007. Arsenic sorption onto natural hematite, magnetite, and goethite. *J. Hazard. Mater.*, 141, 575–580. <https://doi.org/10.1016/j.jhazmat.2006.07.020>.
- Goldberg S., Johnston C.T. 2001. Mechanisms of Arsenic Adsorption on Amorphous Oxides Evaluated Using Macroscopic Measurements, Vibrational Spectroscopy, and Surface Complexation Modeling. *J. Colloid Interface Sci.* 234, 204–216. <https://doi.org/10.1006/jcis.2000.7295>.
- Guillén M. T., Delgado J., Albanese S., Nieto J. M., Lima A. M., De Vivo B. 2012. Heavy metals fractionation and multivariate statistical techniques to evaluate the environmental risk in soils of Huelva Township (SW Iberian Peninsula). *J. Geochem. Explor.* 119–120, (32–43). <https://doi.org/10.1016/j.gexplo.2012.06.009>.
- Haffert L., Craw D. 2008. Mineralogical controls on environmental mobility of arsenic from historic mine processing residues, New Zealand. *Appl. Geochem.* 23, 6, 1467-1483. <https://doi.org/org/10.1016/j.apgeochem.2007.12.030>.
- Hayat K., Menhas S, Bundschuh J., Chaudhar H.J. 2017. Microbial biotechnology as an emerging industrial wastewatertreatment process for arsenic mitigation: A critical review. *J Clean Prod.* 151, 427-438. <https://doi.org/10.1016/j.jclepro.2017.03.084>.
- Larios R., Fernández-Martínez R., Álvarez R. Rucandio I. 2012. Arsenic pollution and fractionation in sediments and mine waste samples from different mine sites. *Sci. Total Environ.* 431, 426-435. <https://doi.org/10.1016/j.scitotenv.2012.04.05>.
- Lata S., Samadde S.R. 2016. Removal of arsenic from water using nano adsorbents and challenges: A review. *J. Environ. Manage*, 166, 387-406. <https://doi.org/10.1016/j.jenvman.2015.10.039>.
- Li Q., Xu X.T., Cui H., Pang J., Wei Z., Sun Z., Zhai J. 2012. Comparison of two adsorbents for the removal of pentavalent arsenic from aqueous solutions. *J. Environ. Manage*, 98, 98-106. <https://doi.org/10.1016/j.jenvman.2011.12.018>.

- Luque Cabal C., Gutiérrez Claverol M. 2006.. La minería de mercurio en Asturias. Rasgos históricos. Oviedo. Eujoa p, 86-336-378-416.
- Luque C. 1985. Las mineralizaciones de Hg de la Cordillera Cantábrica Doct. Thesis. Universidad de Oviedo (unpublished).
- Mamindy-Pajany Y., Hurel C., Marmier N., Roméo M. 2011. Arsenic (V) adsorption from aqueous solution onto goethite, hematite, magnetite and zero-valent iron: Effects of pH, concentration and reversibility. *Desalination* 281, 93–99. <https://doi.org/10.1016/j.desal.2011.07.046>.
- Matanzas N., Sierra M.J., Afif, Díaz T.E. Gallego J. R., Millán R. 2017. Geochemical study of mining-metallurgy site polluted with As and Hg and the transfer of these contaminants to *Equisetum* sp. *J. Geochem. Explor.* 181, 1 – 9. <https://doi.org/10.1016/j.gexplo.2017.08.008>.
- Mazaheri H., Ghaedi M., Ahmadi Azqhandi M.H., Asfaram A. 2017. Application of machine/statistical learning, artificial intelligence and statistical experimental design for the modeling and optimizations of methylene blue and Cd(II) removal from binary aqueous solution by natural walnut carbon. *Phy. Chem. Chem. Phys.*, 19, 11299-11317. <https://doi.org/10.1039/c6cp08437k>.
- Medina A, Gamero P., Almanza J. M., Vargas A., Montoya A., Vargas G., Izquierdo M. 2010. Fly ash from a Mexican mineral coal. II. Source of W zeolite and its effectiveness in arsenic(V) adsorption. *J. Hazard. Mater.*, 181 (1–3), 91-104. <https://doi.org/10.1016/j.jhazmat.2010.04.102>.
- Mukhopadhyay R., Manjaiaha K.M., Datta S.C., Yadav R.K., Sarkar B. 2017. Inorganically modified clay minerals: Preparation, characterization, and arsenic adsorption in contaminated water and soil. *Appl Clay Sci.* 147, 1-10. <https://doi.org/10.1016/j.clay.2017.07.017>.
- Nicomel N.R., Leus K., Folens K., Van Der Voort P., Du Laing G. 2016. Technologies for Arsenic removal from water: current status and future perspectives. *Int J Environ Res Public Health.* 13, 62 <https://doi.org/10.3390/ijerph13010062>.
- Nidheesh P.V., Anantha Singh T.S. 2017. Arsenic removal by electrocoagulation process: Recent trends and removal mechanism. *Chemosphere* 181, 418-432. <https://doi.org/10.1016/j.chemosphere.2017.04.082>.

- Oh C., Rhee S., Oh M., Park J. 2012. Removal characteristics of As(III) and As(V) from acidic aqueous solution by steel making slag. *J. Hazard. Mater.*, 213–214, 147–155. <https://doi.org/10.1016/j.jhazmat.2012.01.074>.
- Rahman S., Kim K.H., Saha SK., Swaraz AM., Paul D.K. 2014. Review of remediation techniques for arsenic (As) contamination: A novel approach utilizing bio-organisms. *J. Environ. Manage*, 134, 175-185. <https://doi.org/10.1016/j.jenvman.2013.12.027>.
- Rieuwerts J.S., Mighanetara K., Braungardt C.B., Rollinson G.K., Pirrie D., Azizi F. 2014. Geochemistry and mineralogy of arsenic in mine wastes and stream sediments in a historic metal mining area in the UK. *Sci. Total Environ.* 472, 226–234. <https://doi.org/10.1016/j.scitotenv.2013.11.029>.
- Rodríguez-Blanco J.D., Jiménez A., Prieto M. 2007. Oriented Overgrowth of Pharmacolite ($\text{CaHAsO}_4 \cdot 2\text{H}_2\text{O}$) on Gypsum ($\text{CaSO}_4 \cdot 2\text{H}_2\text{O}$). *Cryst. Growth Des.* 7, 2756–2763. <https://doi.org/10.1021/cg070222+>.
- Sarkar A., Paul B. 2016. The global menace of arsenic and its conventional remediation- A critical review. *Chemosphere* 158, 37-49. <https://doi.org/10.1016/j.chemosphere.2016.05.043>.
- Siddiqui S., Chaudhry S.A. 2017. Iron oxide and its modified forms as an adsorbent for arsenic removal: A comprehensive e recent advancement. *Protection. Process Saf. Environ. Prot.* 111, 592–626. <https://doi.org/10.1016/j.psep.2017.08.009>.
- Singh R., Singh S., Parihar P., Singh V. P., Prasad S. M. 2015. Arsenic contamination, consequences and remediation techniques: A Review. *Ecotox. Environ. Safe.* 112, 247-270. <https://doi.org/10.1016/j.ecoenv.2014.10.009>.
- Takeo K. 2005. Atlas of Eh-pH diagrams. Intercomparison of thermodynamic databases. Geological Survey of Japan Open File Report No.419. National Institute of Advanced Industrial Science and Technology Research Center for Deep Geological Environments. 30-31, available at http://eosremediation.com/download/Chemistry/.../Eh_pH_Diagrams.pdf
- Ungureanu G., Santos S., Boaventura R., Botelho C. 2015. Arsenic and antimony in water and wastewater: overview of removal techniques with special reference to latest advances in adsorption. *J. Environ. Manage*, 151, 326-342. <https://doi.org/10.1016/j.jenvman.2014.12.051>.

Vidheesh P. V., Anantha Singh T.S. 2017. Arsenic removal by electrocoagulation process: Recent trends and removal mechanism. *Chemosphere* 181, 418-432. <https://doi.org/10.1016/j.chemosphere.2017.04.082>.

Wan X., Dong H., Feng L., Lin Z., Luo Q. 2017. Comparison of three sequential extraction procedures for arsenic fractionation in highly polluted sites. *Chemosphere* 178, 402-410. <https://doi.org/10.1016/j.chemosphere.2017.03.078>.

Wang Y., Tsang D. C. W. 2013. Effects of solution chemistry on arsenic (V) removal by low-cost adsorbents. *J. Environ. Sci.* 25(11) 2291–2298. [https://doi.org/10.1016/S1001-0742\(12\)60296-4](https://doi.org/10.1016/S1001-0742(12)60296-4).

Wu Y., Zhou X-y., Lei M., Yang J., Ma J., Qiao P.-w., Chen T-b. 2017. Migration and transformation of arsenic: contamination control and remediation in realgar mines areas. *Appl. Geochem.* 77, 44-51. <https://doi.org/10.1016/j.apgeochem.2016.05.012>.

www.Asturias.es (accessed on 23/11/2018)

www.chcantabrico.es (accessed on 23/11/2018)

Yang X., Xia L., Li J., Dai M., Yang G., Son S. 2017. Adsorption of As(III) on porous hematite synthesized from goethite concentrate. *Chemosphere* 169, 188-193. <https://doi.org/10.1016/j.chemosphere.2016.11.061>.

Zhang D., Yuan Z., Wang S., Jia Y., Demopoulos G.P. 2015. Incorporation of arsenic into gypsum: Relevant to arsenic removal and immobilization process in hydrometallurgical industry. *J. Hazard. Mater.*, 300, 272–280. <https://doi.org/10.1016/j.jhazmat.2015.07.015>.

Zhu Y.N., Zhang X.H., Xie Q.L., Wang D.Q., Cheng G.W. 2006. Solubility and Stability of Calcium Arsenates at 25°C. *Water Air Soil Pollut.* 169, 221–238. <https://link.springer.com/article/10.1007/s11270-006-2099-y>



Fig. 1. Location of La Soterraña mining and metallurgical site.

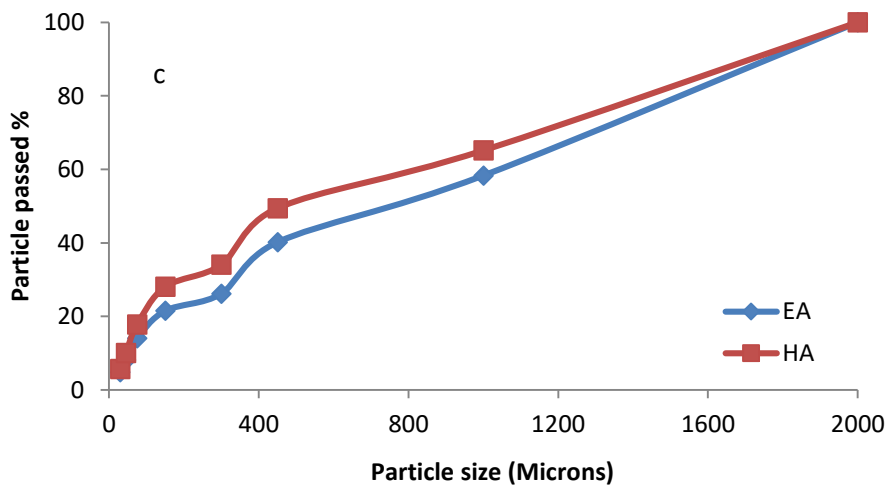
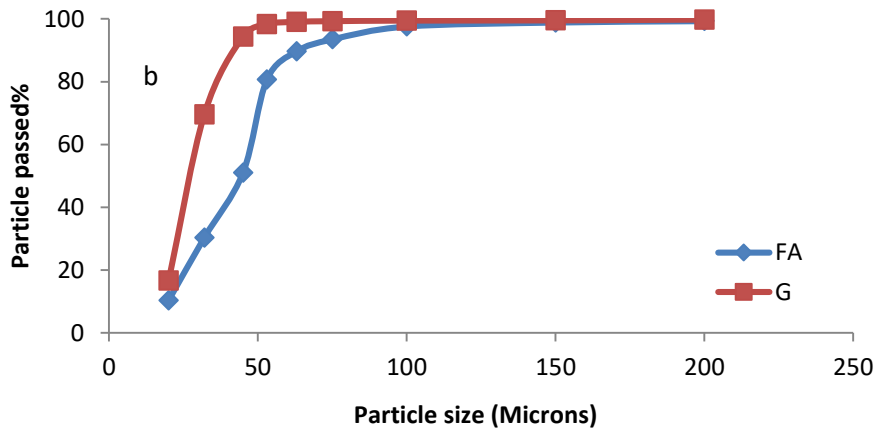
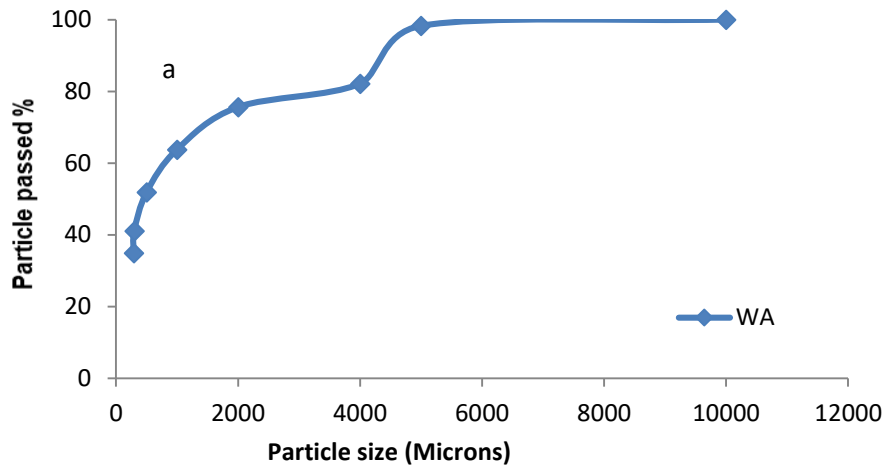
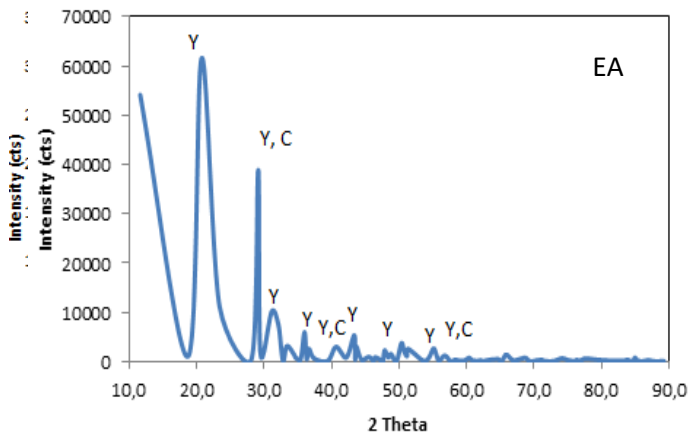
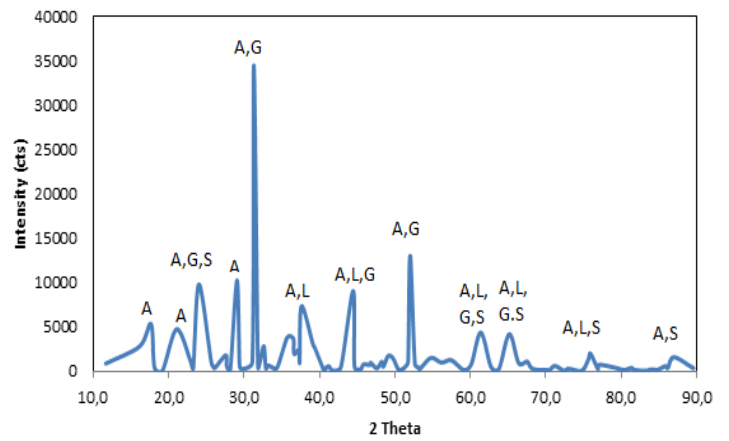
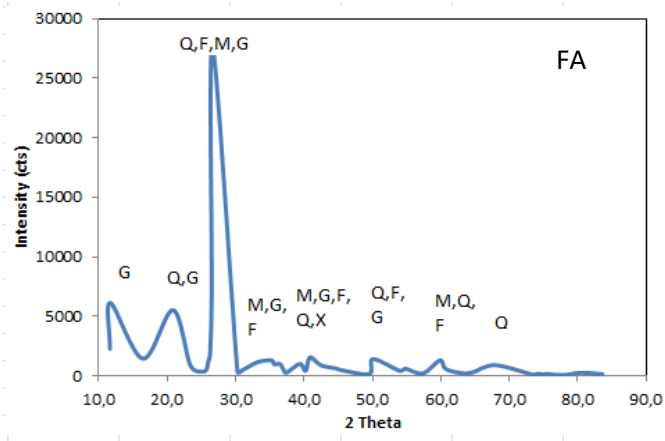


Fig. 2. Particle size distribution: a) La Soterraña waste; b) power plant byproducts; c) steelmaking byproducts.



HA

Fig. 3. X-ray diffraction pattern of the byproducts: M-Mullite (ref 01-074-2419), A-Akermanite (ref 801-076-0841), Q-Quartz (ref 01-089-1961), L-Larnite (ref 01-077-0409), G-Gypsum (ref 01-076-1746), X-Anhydrite, F-Maghemite (ref 01-089-5892), C-Calcite (ref 01-077-1652), S-Srebrodolskite (ref 01-071-2264), P-Portlandite (ref 00-044-1481), W-Merwinite (ref 01-089-2432) and Z-Magnetite (ref 01-089-3854).

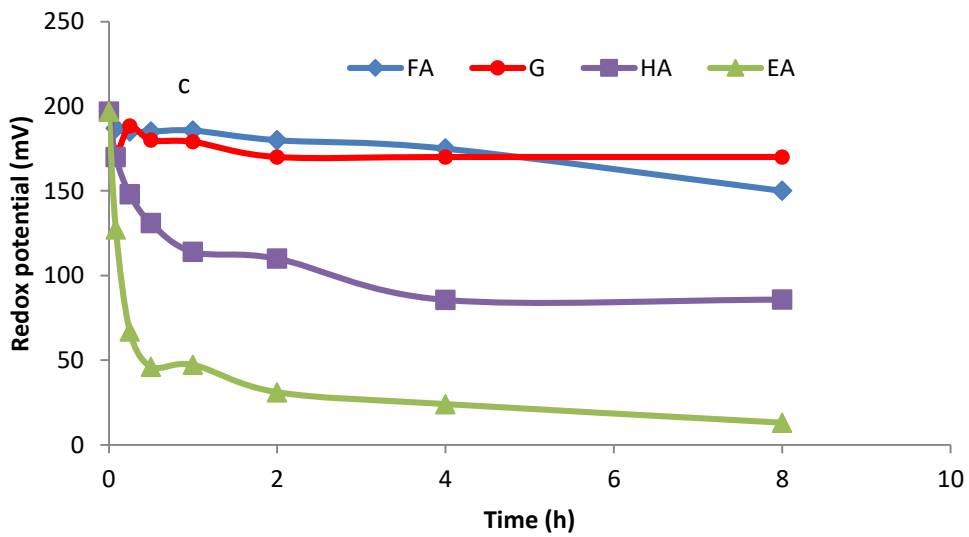
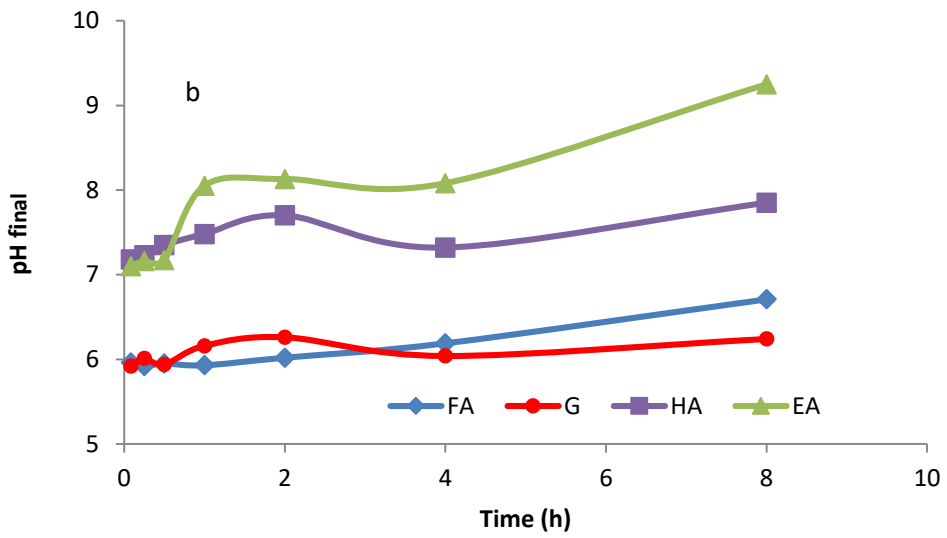
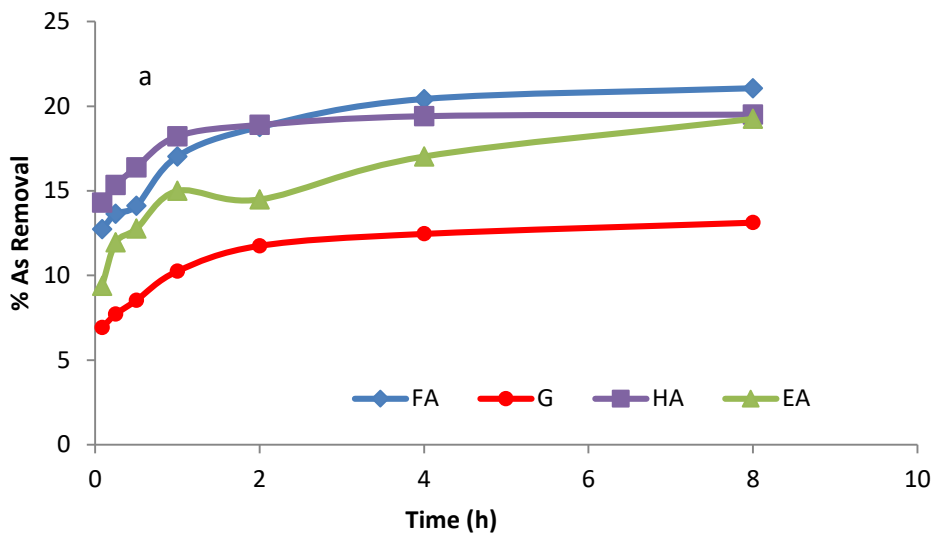


Fig 4. Effect of contact time: a) As removal onto different adsorbents, b) final pH, and c) redox potential.

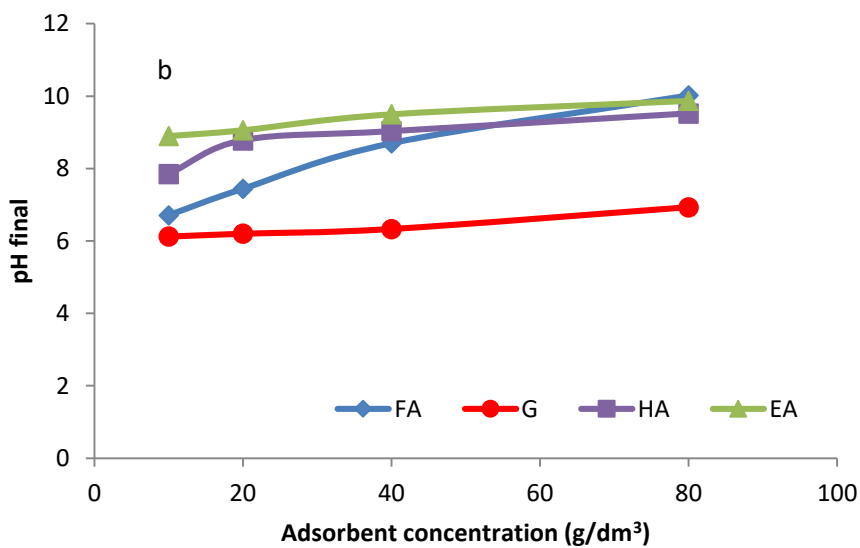
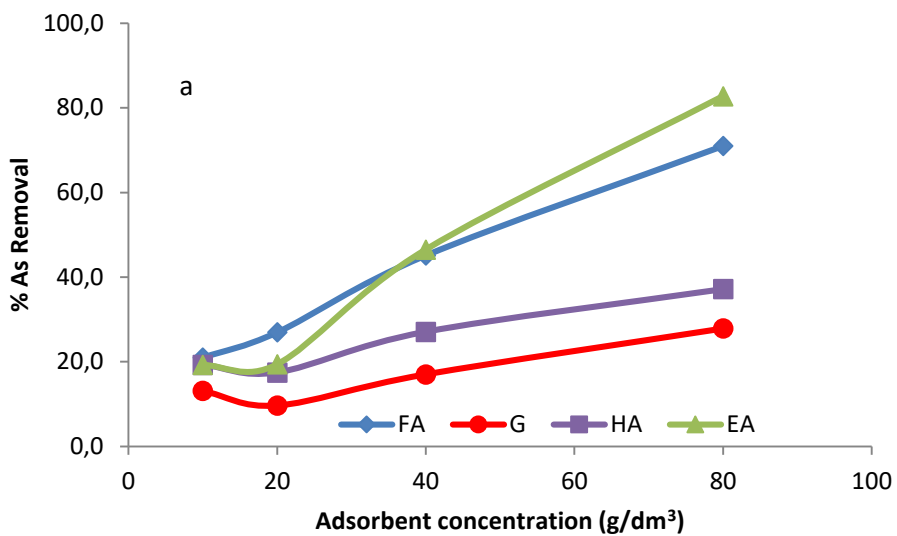
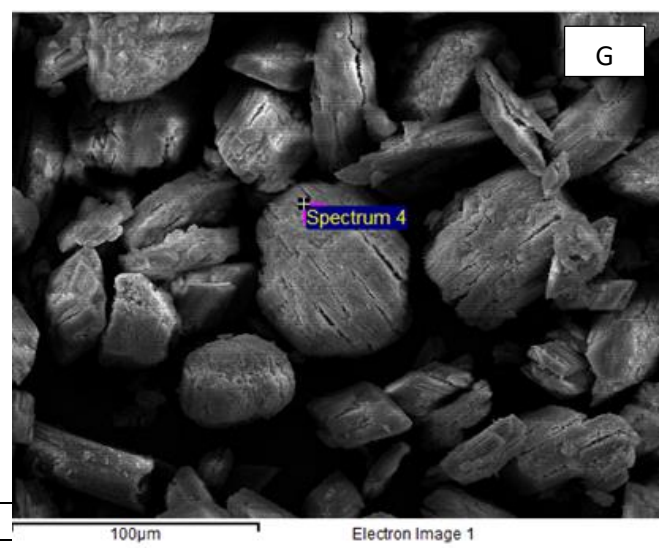
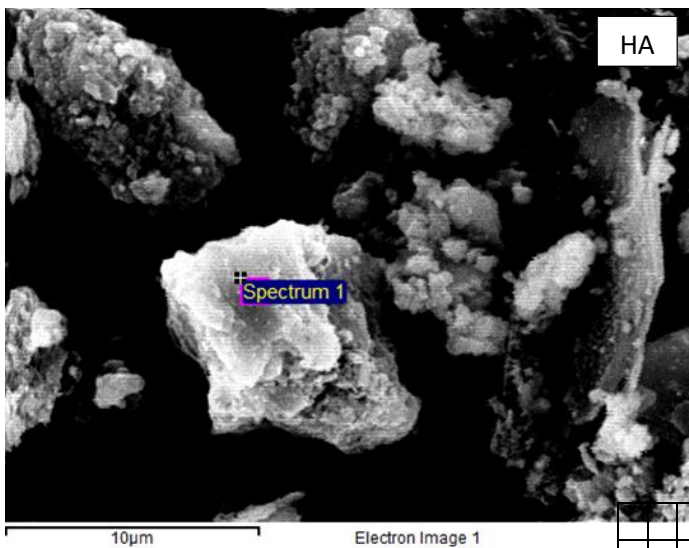
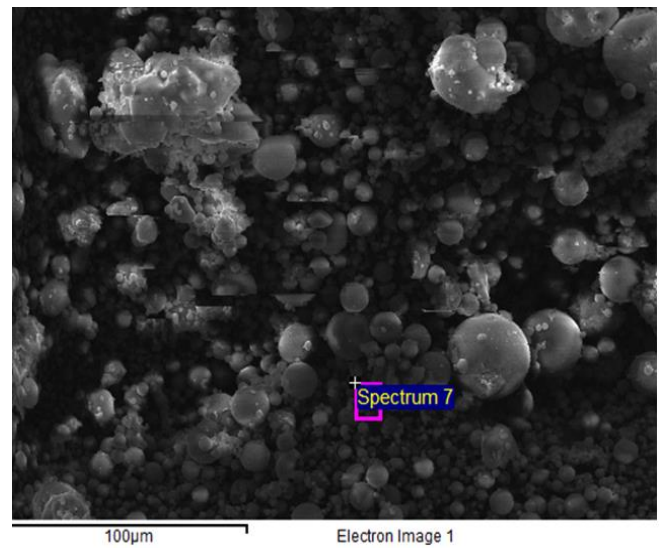
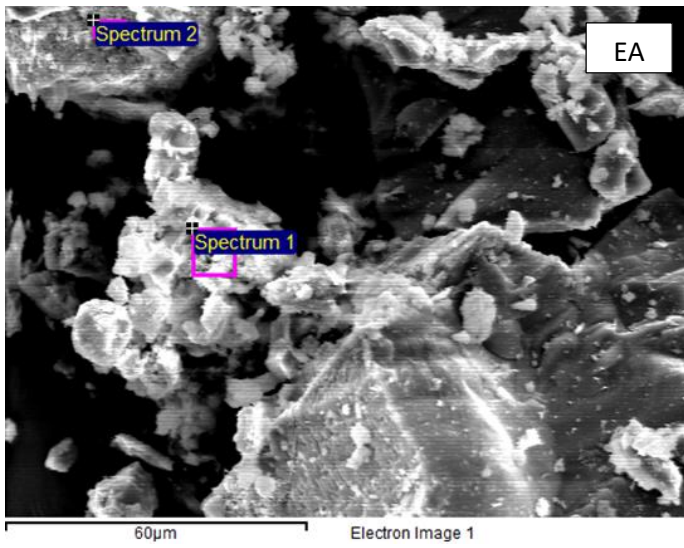


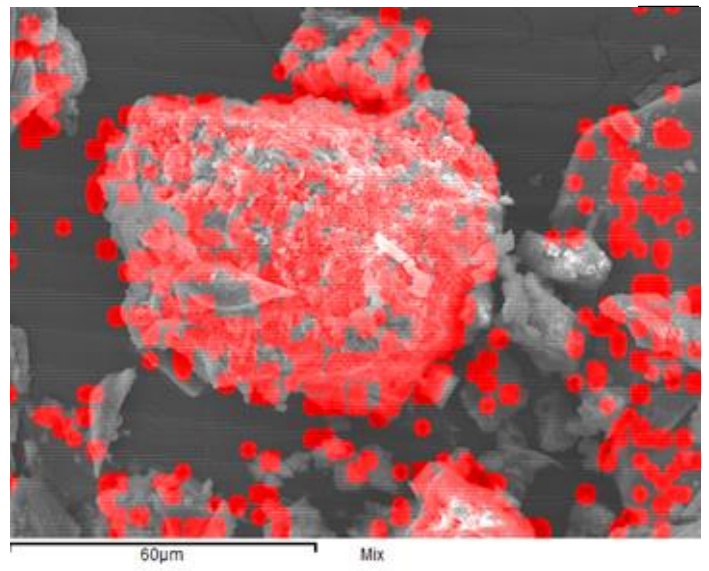
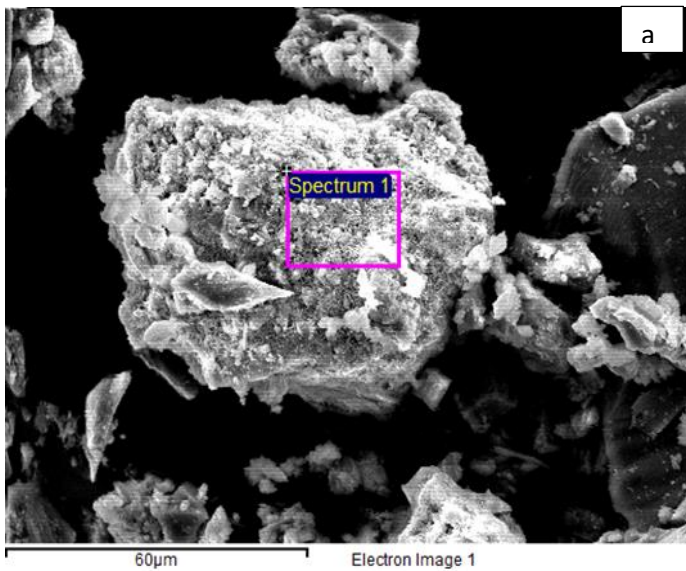
Fig 5. Effect of the adsorbent dosage: a) As removal onto different adsorbents, b) final pH.



Elements analyzed wt%.

Sample	C	O	Na	Mg	Al	S	Si	K	Ca	Ti	Mn	Fe	Cu	As	Au	Total
EA 1	4.57	38.89		2.12	4.99		13.11		27.94				1.62	2.02	4.74	100
EA2	8.40	34.17		1.08	2.47		7.41		34.58		0.83		2.34	1.75	6.97	100
FA	35.49	14.80	0.42	0.45	7.23		15.33	2.87	4.81			7.84	4.32	0.93	5.51	100
HA	7.50	34.42			1.29		1.01		20.14	0.61	1.91	20.28	1.24	1.35	10.25	100
G		27.4				22.02			34.13				3.98	0.46	12.01	100

Fig.6 Scanning electron micrograph and EDX analysis of byproducts after the treatment of the leachate using an adsorbent concentration of 40g/dm³ and stirring for 8 hours.



Processing option : All elements analysed (Normalised)

C

<u>Spectrum</u>	<u>In stats.</u>	C	O	Mg	Al	Si	K	Ca	Ti	Mn	Cu	As	Au	Total
<u>Spectrum 1</u>	Yes	-2.93	45.32	1.00	4.26	11.30	2.16	24.80	3.85	0.97	2.02	1.61	5.64	100.00
Mean		-2.93	45.32	1.00	4.26	11.30	2.16	24.80	3.85	0.97	2.02	1.61	5.64	100.00
<u>Std. deviation</u>		0.00	0.00	0.00	0.00	0.00	0.00	0.00	0.00	0.00	0.00	0.00	0.00	
Max.		-2.93	45.32	1.00	4.26	11.30	2.16	24.80	3.85	0.97	2.02	1.61	5.64	

Fig 7. SEM-EDX analysis after the treatment of the leachate with EA: a) SEM Image, b) SEM-EDX elemental mapping of As, c) SEM-EDX elemental analysis.

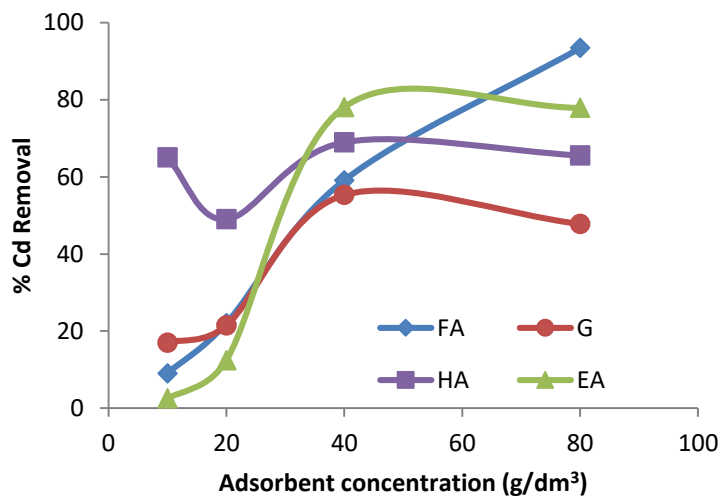
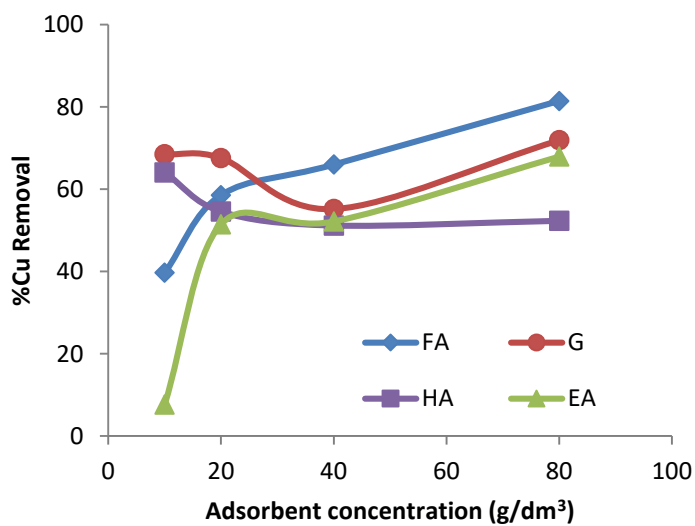
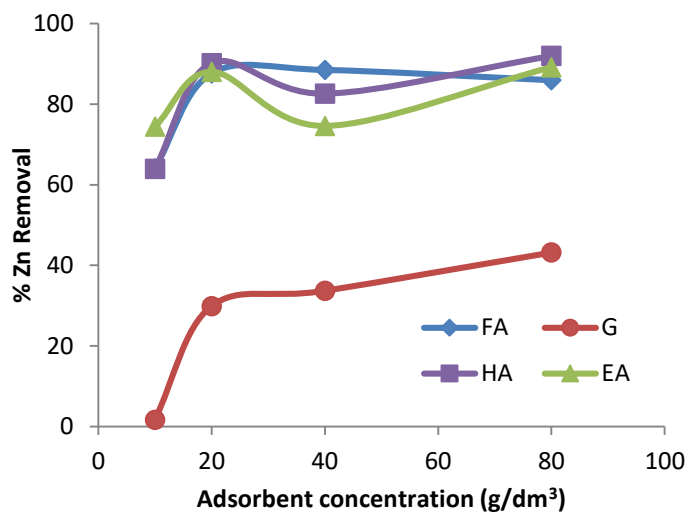
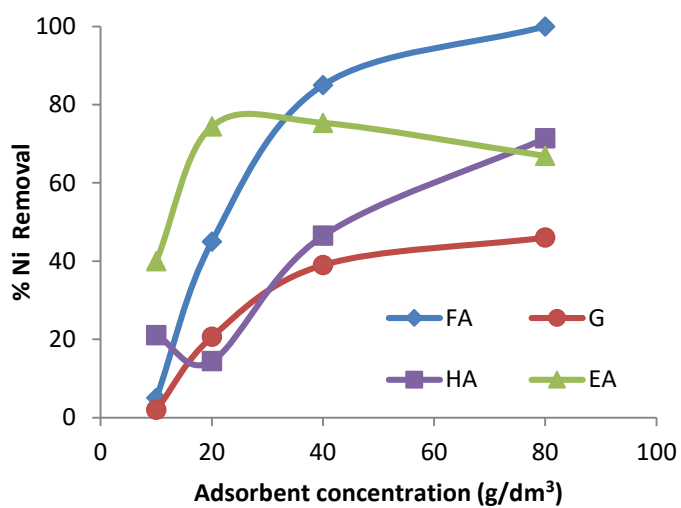


Fig 8. Effect of the adsorbent dosage on the removal of heavy metals.

Table 1. Physico-chemical characteristics of arsenic waste and byproducts.

	WA	FA	EA	HA	G
SiO ₂ (wt%)	61.7	56.5	34.2	13.8	
Fe ₂ O ₃ (wt%)	7.1	9.5	0.34	37.9	
MgO (wt%)		0.9	5.7	1.1	
K ₂ O (wt%)	0.8	2.61	0.44	0.3	
Al ₂ O ₃ (wt%)	7.1	23.9	12.8	2.1	
CaO (wt%)	3.9	3.4	42	38.3	32.5
SO ₃ (wt%)	7.2	2.04	3.29	1.14	46.5
TiO ₂ (wt%)	0.55	0.85	0.64	0.53	
MnO (wt%)	0.02		0.31	3.49	
Hg mg/Kg	34691	2	5.5	16.3	3
As mg/Kg	54801	59	10.3	37.8	1.7
Zn mg/Kg	0.03	90	4	57.5	1.9
Cu mg/Kg	420	57	2.18	26	2.6
Cr mg/Kg	920	83.6	27	49	42.6
Pb mg/Kg	3400	16	1	9	0.6
Ni mg/Kg	0.02	65.4	0.4	24	0.7
Cd mg/Kg	0.01	1.84		0.16	
pH	5.1	10.9	11.3	11.0	7.8
real density g/cm ³		2.38	3.00	3.58	2.51

Table 2. Concentration of toxic elements in the leachate.

Element	Concentration ($\mu\text{g}/\text{dm}^3$)
As	59,057
Hg	0.98
Ni	47.5
Cu	288.6
Zn	107
Pb	10.9
Cd	25.1

Table 3. Comparison of adsorption capacities of various adsorbents for removing As (V) ions reported in literature.

Adsorbent	Qm (mg/g)	Ref.
Magnesia fly ash	0.030	Li et al. (2012)
Maganese fly ash	0.030	Li et al. (2012)
Fly ash	0.4	Balsamo et al. (2010)
Goethite	1.183	Dai et al. (2016)
Siderite	2.37	Dai et al. (2016)
Hematite	0.845	Dai et al. (2016)
Clays	1.076 - 0.56	Bentahar et al. (2016)
Modified clay	0.156	Mukhopadhyay et al. (2017)
Steel byproducts	0.05 - 1.25	Ahn et al. (2003)
Steel-making slag	0.66	Chakraborty et al. (2014)
Steel-making slag	1	Oh et al. (2012)
Fly ash	0.664 - 0.728	Wang et al. (2013)
Lignite	0.655	Wang et al. (2013)
Green waste compost	0.436	Wang et al. (2013)
Zeolites	0.03 - 0.072	Medina et al. (2010)
CV	1.166	Present study
EA	1.069	Present study
HA	1.072	Present study
G	0.728	Present study